Inorganic Chemistry
Article

Inorg. Chem. **2010**, *49*, 1811–1818
DOI: 10.1021/ic9021933

Nanocluster Model of Intermetallic Compounds with Giant Unit Cells: β, β'-Mg_2Al_3 Polymorphs

Vladislav A. Blatov,*[†] Gregory D. Ilyushin,[‡] and Davide M. Proserpio[§]

[†]*Samara State University, Ac. Pavlov St. 1, Samara 443011, Russia,* [‡]*Institute of Crystallography of RAS, Leninsky Pr., 59, Moscow 117333, Russia, and* [§]*Università degli Studi di Milano, Dipartimento di Chimica Strutturale e Stereochimica Inorganica (DCSSI), Via G. Venezian 21, 20133 Milano, Italy*

Received November 6, 2009

A novel method for the computational description of intermetallics as an assembly of nanoclusters was improved and applied to extremely complicated crystal structures of β, β'-Mg_2Al_3 polymorphs. Using the TOPOS program package that implements the method, we separated two types of two-shell primary nanoclusters *A*, *A*1, *A*2, and *B* consisting of 57−63 atoms that completely compose the structures of the polymorphs. The nanocluster model interprets structural disordering in β-Mg_2Al_3: the disordered atoms form the inner shell of the nanocluster *A*, while the outer shells of all nanoclusters are preserved. The self-assembly of the β, β'-Mg_2Al_3 crystal structures was considered within the hierarchical scheme: 0D primary polyhedral clusters (coordination polyhedra) → 0D two-shell primary nanoclusters *A*, *A*1, *A*2, or *B* → 0D supracluster-precursor AB_2 → 1D primary chain → 2D microlayer → 3D microframework. The self-assembly scheme proves the similarity of β, β'-Mg_2Al_3 to other extremely complicated Samson's phases, $NaCd_2$ and $ZrZn_{22}$; the spatial arrangement of the centers of nanoclusters in these structures as well as the topology of the corresponding network conform to the Laves phase $MgCu_2$. Using the TOPOS procedure of searching for finite fragments in infinite nets we found that nanocluster *B* is a typical fragment of intermetallic compounds: it exists in intermetallics belonging to 42 Pearson classes. The nanocluster *A* was found only in two Pearson classes: *cF*464 and *hP*238, while the nanoclusters *A*1 and *A*2 occur in β'-Mg_2Al_3 only. Thus, the nanoclusters *A*, *A*1, and *A*2 can be considered as "determinants" of the corresponding structures.

Introduction

The complexity of some intermetallic compounds is well-known to crystal chemists, and many scientists have attempted to find a common way to describe them; nonetheless, a uniquely accepted descriptive approach to their three-dimensional intricate structures is still lacking.[1,2] Many different descriptions in terms of polyhedron packing have been reported and yet recently Stephen Lee group tackled the "enigma of complex intermetallic structures" via higher dimensional space trying to answer the question: "Is there some pattern to these complex crystal structures that eludes the casual observer, but which can explain essential features of their structures?"[3,4] In contrast, recently we proposed[5−7] a rigorous analytical procedure (*nanocluster method*) that provides a universal and objective approach to modeling of intermetallic compounds of any complexity in real space as an assembly of nanoclusters according to a set of formal criteria. The nanocluster method was algorithmized and implemented into the program package TOPOS[8] that allowed us to apply it to some highly complicated intermetallics. This paper concerns the analysis of intermetallic compounds with giant unit cells to be referred to as Samson's phases.

In 1960s Samson[9−13] determined a number of extremely complicated crystal structures being formed in the binary intermetallic systems Zr−Zn, Na−Cd, Cu−Cd, and Mg−Al. Their formulas are ordinarily written as $ZrZn_{22}$, $NaCd_2$, Cu_4Cd_3, and β-Mg_2Al_3, respectively; however, the last three crystal structures are disordered and have variable composition.

---

*To whom correspondence should be addressed. E-mail: blatov@ssu.samara.ru. Phone: +7-8463345445. Fax: +7-8463345417.

(1) Pearson, W. B. *The Crystal Chemistry and Physics of Metals and Alloys*; Wiley-Interscience: New York, 1972.
(2) Ferro, R.; Saccone, A. *Intermetallic Chemistry*; Pergamon: Oxford, 2008.
(3) Berger, R.; Lee, S.; Johnson, J.; Nebgen, B.; Sha, F.; Xu, J. *Chem.—Eur. J.* **2008**, *14*, 3908.
(4) Berger, R.; Lee, S.; Johnson, J.; Nebgen, B.; So, A.C.-Y. *Chem.—Eur. J.* **2008**, *14*, 6617.
(5) Shevchenko, V. Ya.; Blatov, V. A.; Ilyushin, G. D. *Glass Phys. Chem.* **2009**, *35*, 1.
(6) Shevchenko, V. Ya.; Blatov, V. A.; Ilyushin, G. D. *Struct. Chem.* **2009**, *20*, 975.
(7) Ilyushin, G. D.; Blatov, V. A. *Acta Crystallogr.* **2009**, *B65*, 300.
(8) Blatov, V. A. *IUCr CompComm Newsletter* **2006**, *7*, 4.
(9) Samson, S. *Acta Crystallogr.* **1961**, *14*, 1229.
(10) Samson, S. *Nature* **1962**, *195*, 259.
(11) Samson, S. *Acta Crystallogr.* **1964**, *17*, 491.
(12) Samson, S. *Acta Crystallogr.* **1965**, *19*, 401.
(13) Samson, S. *Acta Crystallogr.* **1967**, *23*, 586.

These structures have attracted strong attention for many years. After the detailed description of them by Samson,[14,15] many alternative models were proposed.[16−21]

Cubic phases of $NaCd_2$, Cu_4Cd_3, and β-Mg_2Al_3 contain large number of inequivalent atoms and totally more than 1000 atoms in the giant (up to 28500 Å^3) unit cell; their Pearson codes are *cF*1192, *cF*1124, and *cF*1168, respectively. Crystallochemical complexity is also high; for instance, $NaCd_2$ as well as an ordered model of β-Mg_2Al_3 contains 672 icosahedra (**ico**),[22] 252 Friauf polyhedra (with 16 vertices and 28 triangular faces observed by Friauf in $MgCu_2$ and also called **mcp**)[23], and 244 other polyhedra with 13, 14, or 15 vertices and only has one partially occupied atomic position. However, unlike $NaCd_2$, 11 out of 23 atomic positions occupied in β-Mg_2Al_3 are split because of disordering. To describe the disordered model of β-Mg_2Al_3, Pearson[1] introduced a special type of coordination polyhedron that is based on a pentagonal prism and has four additional vertices. Note that after Pearson all other authors considered an ordered model of β-Mg_2Al_3 that topologically coincides with $NaCd_2$ (hereafter we call this ordered model as $NaCd_2/\beta$-Mg_2Al_3). Recently, a large international team[20] refined β-Mg_2Al_3 and determined that it undergoes at 214 °C a first-order phase transition to a low-temperature rhombohedral phase, β'-Mg_2Al_3 (*hR*293). They showed that β'-Mg_2Al_3 is structurally close to β-Mg_2Al_3, but in contrast to it is not positionally disordered.

The cause of the principal difficulties in the topological description of such complicated intermetallic compounds is that they cannot be represented as a packing of planar networks[1], and, hence, some cluster (polyhedral) models should be applied. Thus, Samson[11−13] separated the cyclic structural blocks consisting of five icosahedra or of five Friauf polyhedra in the structures of Cu_3Cd_4 or $NaCd_2$, respectively. In $NaCd_2/\beta$-Mg_2Al_3 these 47-atom blocks are fused in a more complex cluster composed of 234 atoms. This cluster has high local symmetry $\overline{4}3m$ (it occupies Wyckoff position 8*a* of the space group $Fd\overline{3}m$), and its center is empty. It contains 15 out of 17 crystallographically inequivalent atoms; the remaining two atoms (Na and Cd) are spacers. The Na atoms occupy 8*b* positions, and these atoms together with the cluster centers form two interpenetrating diamond sublattices. Totally, 1152 out of the 1192 atoms composing the unit cell are included into the Samson 234-atom clusters. However, this model raises some problems as follows.

(i) The average number of atoms per cluster in the unit cell is 1152/8 = 144, that is, the 234-atom cluster shares a large number (90) of atoms at the condensation. This casts doubt that the clusters really exist in the melted phase.

(ii) There are other methods of selecting clusters even with other Friauf polyhedra.[17−19] Moreover, clusters can be based on polyhedra of other types, in particular, on icosahedra.[7]

(iii) Not all atoms of the structure are included into the clusters.

Note that while different models for $NaCd_2$[17−19] and Cu_3Cd_4[16] were proposed after Samson′s original investigations, for β-Mg_2Al_3 the Samson model was retained in the last X-ray redetermination performed.[20]

Recently,[6] we used the nanocluster method to describe the structure of $NaCd_2$ as an assembly of two-shell 61-atom and 63-atom nanoclusters, whose centers are arranged over the positions of the $MgCu_2$ Laves phase. Unlike other models of $NaCd_2$, the nanoclusters include all atoms of the structure. We showed[7] that the structures of the $ZrZn_{22}$ family are assembled of nanoclusters AX_{16} (Friauf polyhedron) and BX_{12} (icosahedron) united into cyclic supraclusters AB_2X_{37}; this model explains the superstructure ordering in $Mg_3Ti_2Al_{18}$ and $CeCr_2Al_{20}$ belonging to the $ZrZn_{22}$ family. Below we use the nanocluster method to model the self-assembly of the Samson phase β-Mg_2Al_3 and its low-temperature polymorph β'-Mg_2Al_3, and we compare it with the other models described below.

Principles of the Nanocluster Analysis. To construct the models of β-Mg_2Al_3 and β'-Mg_2Al_3 we have used the improved algorithm[7] that is based on the following principles:

(i) The crystal structure is assembled of a small set of *primary* nanoclusters corresponding to stable atomic configurations that, in general, have multishell (onion) architecture. The topology of the cluster is determined by the so-called shell graph SG_n;[24] the atoms of the *n*th shell are called *external*, atoms of other shells are referred to as *internal*. The configurations are assumed to be stable if they occur in intermetallic compounds of other types. Interconnected centers of the primary nanoclusters form an *underlying net* that is as a rule much simpler than the net of the structure under consideration.

(ii) The primary nanoclusters have the highest symmetry (occupy the Wyckoff positions with the smallest multiplicity).

(iii) The primary nanoclusters are ordinarily centered with high-coordinated atoms. However, the center of the primary nanocluster can be empty if it obeys the previous principle; in this case, it corresponds to a void.

(iv) The primary nanoclusters cannot have common internal atoms (interpenetrate), but can have common external atoms.

---

(14) Samson, S. *Structural Chemistry and Molecular Biology*; Rich, A., Davidson, N., Ed.; Freeman: New York, 1968; p 687.

(15) Samson, S. *Developments in the Structural Chemistry of Alloy Phases*; Giessen, B. C., Ed.; Plenum Press: New York, 1969; p 65.

(16) Andersson, S. *Acta Crystallogr.* **1980**, *B36*, 2513.

(17) Yang, Q.-B.; Andersson, S.; Stenberg, L. *Acta Crystallogr.* **1987**, *B43*, 14.

(18) Bergman, G. *Acta Crystallogr.* **1996**, *B52*, 54.

(19) Fredrickson, D. C.; Lee, S.; Hoffmann, R. *Angew. Chem., Int. Ed.* **2007**, *46*, 1958.

(20) Feuerbacher, M.; Thomas, C.; Makongo, J. P. A.; Hoffmann, S.; Carrillo-Cabrera, W.; Cardoso, R.; Grin, Y.; Kreiner, G.; Joubert, J.-M.; Schenk, T.; Gastaldi, J.; Nguyen-Thi, H.; Mangelinck-Noël, N.; Billia, B.; Donnadieu, P.; Czyrska-Filemonowicz, A.; Zielinska-Lipiec, A.; Dubiel, B.; Weber, T.; Schaub, P.; Krauss, G.; Gramlich, V.; Christensen, J.; Lidin, S.; Fredrickson, D.; Mihalkovic, M.; Sikora, W.; Malinowski, J.; Brühne, S.; Proffen, T.; Assmus, W.; de Boissieu, M.; Bley, F.; Chemin, J.-L.; Schreuer, J.; Steurer, W. *Z. Kristallogr.* **2007**, *222*, 259.

(21) Wolny, J.; Kozakowski, B.; Duda, M.; Kusz, J. *Phil. Mag. Lett.* **2008**, *88*, 501.

(22) For the three-letter nomenclature of polyhedra and nets see Reticular Chemistry Structure Resource, http://rcsr.anu.edu.au/, and O'Keeffe, M.; Peskov, M. A.; Ramsden, S. J.; Yaghi, O. M. *Acc. Chem. Res.* **2008**, *41*, 1782.

(23) Samson, S. *Acta Crystallogr.* **1958**, *11*, 851.

(24) Blatov, V. A.; Proserpio, D. M. *Acta Crystallogr.* **2009**, *A65*, 202.

Table 1. Correspondences between the Atoms in the β-Mg_2Al_3 and $NaCd_2$ Crystal Structures[a]

β-Mg_2Al_3 (Feuerbacher et al., 2007)			$NaCd_2$ (Samson, 1962)			
atom	occupancy	Wyckoff position	atom	occupancy	Wyckoff position	functional role
Mg(23)	1	8*b*	Na(1)	1	8*b*	central atom of nanocluster *A*
*Al(7)	0.525	96*g*	Cd(8)	0.62Cd+0.38Na	96*g*	first shell of nanocluster *A*
*Al(8)	0.220	96*g*	Cd(8)	0.62Cd+0.38Na	96*g*	first shell of nanocluster *A*
*Al(9)	0.167	96*g*	Cd(8)	0.62Cd+0.38Na	96*g*	first shell of nanocluster *A*
*Al(10)	0.104	96*g*	Cd(8)	0.62Cd+0.38Na	96*g*	first shell of nanocluster *A*
°Al(20)	0.130	96*g*	Na(3)	0.84Na+0.16Cd	32*e*	first shell of nanocluster *A*
°Mg(19)	0.21	96*g*	Na(3)	0.84Na+0.16Cd	32*e*	first shell of nanocluster *A*
Al(14)+Mg(13)	0.61 + 0.39	96*g*	Cd(9)	1	96*g*	second shell of nanocluster *A*
Mg(11)+Al(12)	0.69 + 0.31	96*g*	Na(7)	1	96*g*	second shell of nanocluster *A*
Mg(18)	1	32*e*	Cd(3)	1	32*e*	second shell of nanocluster *A*
Al(21)	0.481	32*e*	Cd(4)	0.5	32*e*	second shell of nanocluster *A*
Mg(6)	1	96*g*	Na(6)	1	96*g*	second shell of nanoclusters *A* and *B*
Al(22)	1	16*c*	Cd(1)	1	16*c*	Central atom of nanocluster *B*
Al(3)	1	96*g*	Cd(6)	1	96*g*	first shell of nanocluster *B*
Mg(4)	1	96*g*	Na(5)	1	96*g*	first shell of nanocluster *B*
Al(1)	1	192*i*	Cd(10)	1	192*i*	second shell of nanocluster *B*
Al(2)	1	96*h*	Cd(5)	1	96*h*	second shell of nanocluster *B*
Al(5)	1	96*g*	Cd(7)	1	96*g*	second shell of nanocluster *B*
Al(16)	1	32*e*	Cd(2)	1	32*e*	second shell of nanocluster *B*
Mg(17)	1	32*e*	Na(2)	1	32*e*	second shell of nanocluster *B*
Mg(15)	1	48*f*	Na(4)	1	48*f*	second shell of nanocluster *B*

[a] *,° are atoms positionally disordered, see section on "Nature of Structural Disordering" for details.

(v) The primary nanoclusters should include all atoms of the crystal structure. In special cases there can be separate atoms (spacers) that can be formally considered as monatomic primary clusters.

(vi) The primary nanoclusters glue into *supraclusters* by sharing or (more preferable) interconnecting external atoms. The entire crystal is formed by a complementary condensation of the identical supraclusters into microchains. A successive condensation of microchains gives rise to microlayers and finally to a microframework (three-dimensional supraprecursor) that predetermines the topology of the underlying net and the subsequent growth of the crystal.

(vii) If several inequivalent models obey principles (i)–(vi), all of them should be more analyzed with accounting additional reasons. An important criterion could be the *parsimony* principle or Ockham's Razor principle:[25] the favorite model should be assembled from the minimum number of primary nanoclusters. The resulting underlying net has the smallest number of inequivalent nodes and can likely have some well-known topology.

Results and Discussion

Topological Characteristics of Nodes of the 3D Nets. First we consider the cubic phase of β-Mg_2Al_3[20] compared to $NaCd_2$.[10] In the crystal structure of β-Mg_2Al_3 there are 10 atoms having abnormally short interatomic distances that can be considered as a superposition of different substructures (Table 1; hereafter the names of shared positions as well as numbers of atoms correspond to the original papers). For β-Mg_2Al_3 we used the data obtained at ambient temperature;[20] the structure determined at 400 °C can be described in the same way.

Table 2. Coordination Sequences for 17 Inequivalent Atoms in $NaCd_2$/β-Mg_2Al_3

atom	Wyckoff position	N_1	N_2	N_3	N_4
Cd(1)/Al(22)	16*c*	12	50	120	212
Cd(2)/Al(16)	32*e*	12	50	109	209
Cd(5)/Al(2)	96*h*	12	49	118	214
Cd(6)/Al(3)	96*g*	12	50	113	213
Cd(7)/Al(5)	96*g*	12	50	114	213
Cd(8)/Al(7–10)	96*g*	12	50	113	214
Cd(10)/Al(1)	192*i*	12	51	118	218
Cd(4)/Al(21)	32*e*	13	46	110	209
Cd(9)/Al(14)Mg(13)	96*g*	13	48	118	214
Na(3)/Al(20)Mg(19)	32*e*	14	55	118	203
Cd(3)/Mg(18)	32*e*	14	55	124	217
Na(7)/Al(12)Mg(11)	96*g*	15	49	113	223
Na(1)/Mg(23)	8*b*	16	44	116	198
Na(2)/Mg(17)	32*e*	16	50	118	223
Na(4)/Mg(15)	48*f*	16	52	127	225
Na(5)/Mg(4)	96*g*	16	52	119	224
Na(6)/Mg(6)	96*g*	16	55	119	228

Using TOPOS we built the ordered model of β-Mg_2Al_3 by merging close partially occupied positions (see for more details the section on "Nature of Structural Disordering"). We assume that the couples of atoms Al(14)/Mg(13) and Al(12)/Mg(11) occupy statistically the same positions because the distances between them are very short (< 0.7 Å) and the sum of occupancies is equal 1. The resulting model is, in fact, a topological analogue of $NaCd_2$, where only site substitutional disorder exists. Thus, in our modeling the 3D net of $NaCd_2$/β-Mg_2Al_3 with 17 occupied Wyckoff positions will be used (Wyckoff symbol is ihg^7fe^5cb, Pearson symbol is $cF1192$ if all the Wyckoff positions are considered completely occupied). In Table 2 coordination sequences $\{N_k\}$, $k = 1-4$, are given for all inequivalent atoms in $NaCd_2$/β-Mg_2Al_3. According to Table 2 the most high-coordinated nodes have $N_1 = 16$ and $N_2 = 44-55$; the most symmetrical positions (8*b*) are occupied by

---

(25) Hoffmann, R.; Minkin, V. I.; Carpenter, B. K. *Bull. Soc. Chim. Fr.* **1996**, *133*, 117.

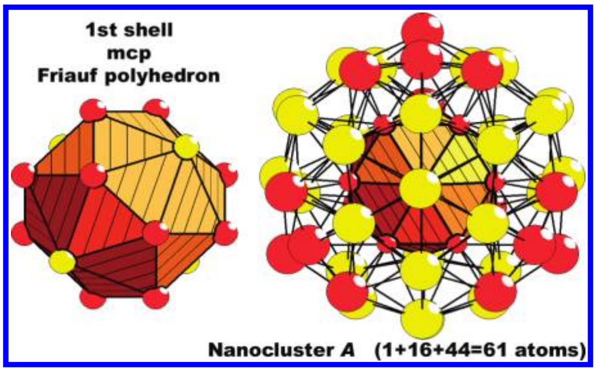

Figure 1. (left) First shell (16 atoms − Friauf polyhedron **mcp**) and (right) the entire nanocluster *A* with 44-atom second shell in the crystal structure of β-Mg_2Al_3 (ordered $NaCd_2$ type model). Hereafter Mg and Al atoms are shown as yellow and red balls, respectively.

Na(1)/Mg(23). Since all nodes have different coordination sequences $\{N_k\}$, they are topologically inequivalent and, hence, play different roles in the 3D nets. These roles are described in Table 1 and will be considered in detail below.

Comparison of corresponding atoms in β-Mg_2Al_3 and $NaCd_2$ (Table 1) results in the following conclusions:

(i) all Na atoms have analogues among Mg atoms;
(ii) in both structures there are positions 32*e* half-occupied by Cd(4)/Al(21);
(iii) atoms Mg(19)/Al(20) are disordered over three 96*g* positions around a 3-fold axis with distances 0.687 Å; the corresponding Na atoms lie on the axis;
(iv) atom Mg(18) corresponds to Cd(3), not to a Na atom; that is one of the reasons of stoichiometric difference between β-Mg_2Al_3 and $NaCd_2$.

Voids. The last edition of the nanocluster method[7] stated the possibility of existence of primary nanoclusters with unoccupied centers but did not define the way to reveal them. In this work we have improved this step of algorithm with the tiling approach[26] that allows one to find all "topological cages" in a net irrespective of their size and geometrical distortion, and, hence, to determine all possible empty centers of nanoclusters. In $NaCd_2$ as well as in the ordered β-Mg_2Al_3 the 3D nets contain 54 inequivalent cages, all of them are tetrahedral, and most of them occupy low-symmetrical positions with multiplicity 32−192. There is the only a high-symmetrical cage with the center in the Wyckoff position 8*a* corresponding to the center of the Samson 234-atom cluster. The sizes of all cages are too small to hold Na or Cd atoms.

Primary Nanoclusters. Primary Nanocluster A. In accord to the principles of the nanocluster analysis, in the first step we have to find the centers of the primary nanoclusters that should coincide with the high-symmetrical high-coordinated atoms or voids. The atoms Mg(23)/Na(1) (position 8*b*) as well as cages centered on the positions 8*a* (they were found in the previous part) obey these conditions. Thus, there are two ways to construct the model: starting from centered (8*b*) or "empty" cluster (around 8*a*). Let us consider the first way.

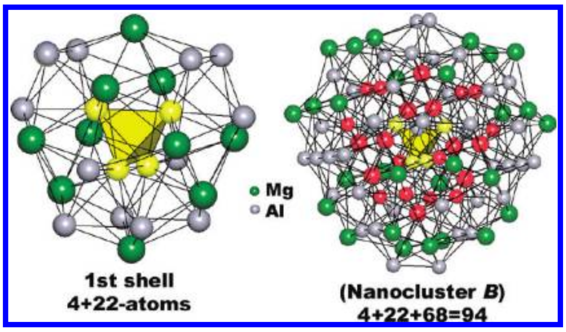

Figure 2. First method of choosing nanocluster *B* in the crystal structure of β-Mg_2Al_3 (ordered $NaCd_2$-type model): (left) first 22-atom shell and (right) the entire nanocluster *B* with 68-atom second shell based on the tetrahedral cage (yellow).

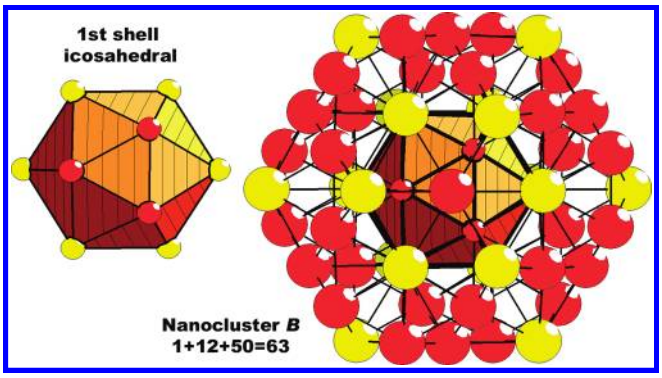

Figure 3. Second method of choosing nanocluster *B* in the crystal structure of β-Mg_2Al_3 (ordered $NaCd_2$-type model): (left) first (icosahedral) shell and (right) the entire nanocluster *B* with 50-atom second shell.

To determine the size of the primary nanocluster we model its shell growth until the equivalent clusters intersect each other. Repeating the growth starting from centered (position 8*b*) two times we obtain a two-shell primary quasi-spherical nanocluster *A* of about 12 Å diameter consisting of $1 + 16 + 44 = 61$ atoms [in β-Mg_2Al_3 they include inequivalent Mg(6), Mg(11), Mg(18), Mg(19), Mg(23) and Al(7), Al(14), Al(21) atoms; for corresponding atoms in $NaCd_2$ see Table 1] (Figure 1). The primary nanoclusters *A* have no shared atoms with other nanoclusters *A* but have common external atoms with nanoclusters *B* (see below).

Primary Nanocluster B. Then we repeat the procedure for the atoms and voids not included into the nanocluster *A*. There are two methods to choose the center of nanocluster *B*.

(i) In the most symmetrical position (8*a*) occupied by the cage surrounded by the tetrahedron of atoms Al(16). The shell growth around the tetrahedron gives two coordination shells consisting of 22 [12Al(3), 6Mg(15), 4Mg(17)] and 68 [24Al(1), 12Al(5), 4Al(22), 24Mg(4), 4Mg(18)] atoms, respectively, that is, the "empty" primary nanocluster is composed of $4 + 22 + 68 = 94$ atoms (Figure 2). There remains the atom Al(2) not belonging to the primary nanoclusters *A* and *B*; this atom has icosahedral environment and should be considered as a spacer.
(ii) In the most symmetrical positions occupied by the atoms not belonging to the primary nanocluster *A*. They are atoms Al(22) with CN = 12 allocated in

---

(26) Blatov, V. A.; Delgado-Friedrichs, O.; O'Keeffe, M.; Proserpio, D. M. *Acta Crystallogr.* **2007**, *A63*, 418.

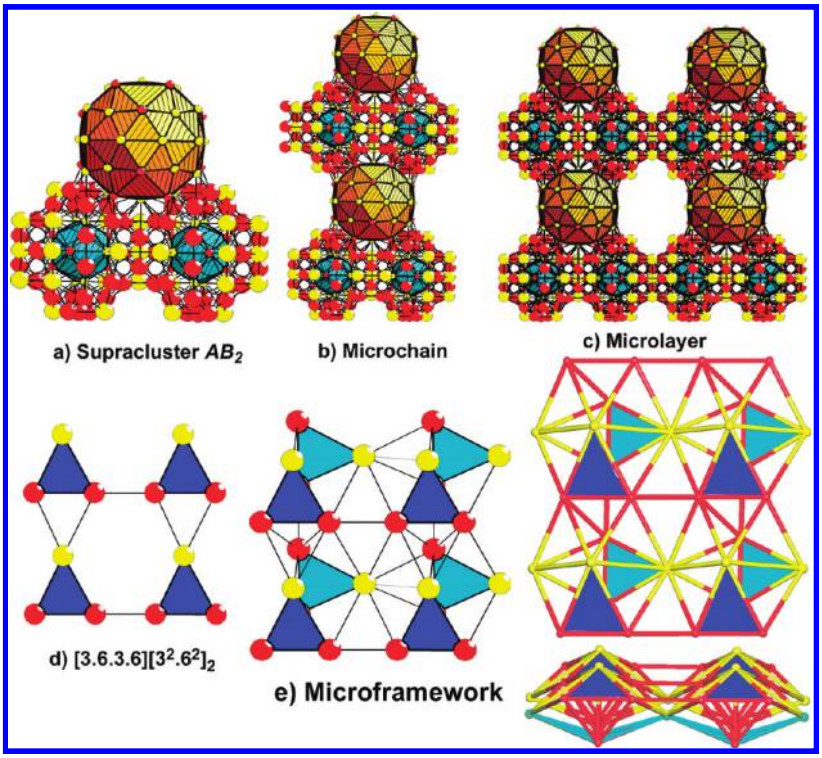

Figure 4. (a) Supracluster-precursor AB_2; (b) assembling the supraclusters into a microchain; (c) assembling the microchains into a microlayer; (d) the resulting plane binodal net $[3.6.3.6][3^2.6^2]_2$; (e) assembling the microlayers into a microframework. Triangular supraclusters are shaded.

positions 16*c*. The shell growth leads to a two-shell nanocluster of about 13 Å diameter composed of 63 atoms (1 + 12 + 50, Figure 3). This primary nanocluster *B* contains all remaining inequivalent atoms, not belonging to the nanocluster *A*, so no spacers occur in this model. It has common external atoms both with other primary nanoclusters *B* [five atoms: 2Al(5)+Mg(15)+2Mg(17)] and with clusters *A* [one atom Mg(18)].

These two methods give rise to two possible models of β-Mg_2Al_3, where the nanocluster *A* is combined with the 94-atom nanocluster and a spacer, or with the 63-atom nanocluster *B*. It is easy by computation to ascertain that all other possible ways of selecting primary nanoclusters in accord to principles of the nanocluster analysis (i)−(v) (in particular, selecting the cage in the position 8*a* as a center of the nanocluster *A*) give rise to one of these two models. The second model (with the 63-atom nanocluster *B*) is preferred according to principle (v) (there are no spacers in it). This model coincides with the model proposed recently[6] and will be used further.

Method of Self-Assembly. The centers of the primary nanoclusters *A* and *B* form an underlying net AB_2 with the topology of the Laves phase $MgCu_2$ (net **mgc-x**). Note that the structural resemblance of the Laves phase and $NaCd_2$ or β-Mg_2Al_3 was many times mentioned before (see[20] and references therein), but only at the atomic level, as the topological resemblance of atomic blocks to be cut in the structures. Now we see that the structures under consideration are similar to $MgCu_2$ at the nanocluster level as well. The structures can be assembled of the primary nanoclusters according to the following hierarchical scheme that is also valid for $MgCu_2$.

Supracluster-precursor AB_2 consists of three primary nanoclusters united into a cycle (Figure 4a). The supracluster has the symmetry *m*, its center occupies a 96*g* position. It is the minimal part of the structure that can grow it by successive translational complementary replication giving intermediate low periodic ensembles: microchains and microlayers.

Microchain is undulated and assembled in a diagonal direction of the cubic unit cell (Figure 4b). Two primary nanoclusters *B* of the same AB_2 nanocluster-precursor link with the primary nanocluster *A* of another nanocluster-precursor by the "key-lock" method. Since the distance between the centers of nanocluster-precursors corresponds to a half of the unit cell diagonal *d*, the sizes of primary nanoclusters predetermine the translation *a* ($d^2 = 2a^2$).

Microlayer is formed of the parallel microchains by uniting their vertices in the perpendicular direction (Figure 4c). The resulting undulated binodal net (Figure 4d) is equivalent to the binodal 4,4-coordinated plane net AB_2 likely first observed in β-W (net **bte**),[27] with the vertex symbol $[3.6.3.6][3^2.6^2]_2$,[28] and has been also found in the $ZrZn_{22}$ crystal structure,[7] but with different kind of *A* and *B* clusters: 1 + 12 and 1 + 16 instead of 1 + 12 + 50 and 1 + 16 + 61, see the section "β, β'-Mg_2Al_3 versus $ZrZn_{22}$".

Three-dimensional microframework can be obtained from the microlayers by their stacking ABCDABCD... along the perpendicular direction with 90° rotation (Figure 4e). This model differs from the building of three-dimensional β-W by that the stacking layers are

---

(27) O'Keeffe, M.; Hyde, B. G. *Phil. Trans. R. Soc. London A*. **1980**, *295*, 553.

(28) For nomenclature see: Blatov, V. A.; O'Keeffe, M.; Proserpio, D. M. *CrystEngComm*. **2010**, *12*, 44.

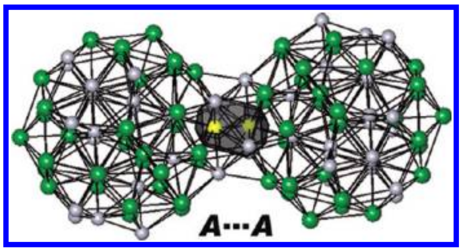

Figure 5. Two nanoclusters *A* connecting with each other in the ordered model of β-Mg_2Al_3. Al and Mg atoms are gray and green, respectively; Al(21) positions are yellow. The cavity between the nanoclusters that includes two half-occupied Al(21) positions is approximated by a black polyhedron that is the Voronoi polyhedron with the center in the middle of the yellow positions.

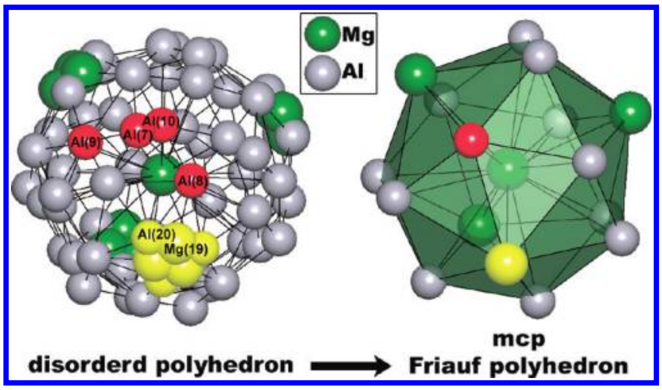

Figure 6. First shell of a nanocluster *A* in β-Mg_2Al_3: (left) disordered model; (right) ordered model. The coordinates of averaged positions in AX_{16} Friauf polyhedron (**mcp**) are as follows: Mg(32*e*), 0.3113, 0.3113, 0.3113; Al(96*g*), 0.0926, 0.0926, 0.5220. Two groups of disordered atoms and corresponding atoms in the ordered model are shown in red (gray) and yellow (green).

undulated and compose the whole structure, while in β-W/**bte** there are other atoms (arranged as 4^4-**sql**) between the stacking ABAB... layers.[1] The microframework consists of eight suprapolyhedral nanocluster-precursors ($4AB_2$+$4AB_2$); it can be considered as a minimal 3D nucleus that predetermines subsequent growth of the crystal macrostructure.

Nature of Structural Disordering. As was mentioned above, the structures of β-Mg_2Al_3 and $NaCd_2$ are disordered differently, but these differences were not analyzed in all earlier cluster models. Below we consider the disordering in relation to the nanocluster model.

(i) The Cd(4)/Al(21) atoms occupying 32*e* positions with about 50% probability are allocated on the surface of the primary nanoclusters *A* in the place of their mutual contact; the distance between the split positions is 2.30/1.98 Å. There is a large cavity in this place (Figure 5), whose volume (21.0 Å^3) exceeds the volume of Al in element (16.6 Å^3) but is less than the volume of two Al atoms ($21.0 < 33.2$ Å^3) that likely gives rise to the disordering.

(ii) Two 96*g* positions in the outer shell of the cluster *A* are shared by pairs Al(12)/Mg(11) and Al(14)/Mg(13) that are substitutionally disordered (Table 1).

(iii) Positional disordering occurs only in the crystal structure of β-Mg_2Al_3; all disordered positions (96*g*) are partially occupied by the atoms Al(7)$-$Al(10), Al(20), and Mg(19) (Table 1). All these atoms lie on the surface of a sphere of about 3 Å radius (Figure 6, left) and form a disordered shell around Mg(23). They can be conditionally transformed into a the Friauf polyhedron that is the core of the primary nanocluster *A* in the ordered model in several ways, for example, by contracting two groups of disordered atoms: Al(20), Mg(19) and Al(7)$-$Al(10) into 32*e* and 96*g* positions, respectively (Figure 6, right). Of course, this consideration is relative and only shows the resemblance of β-Mg_2Al_3 and $NaCd_2$ crystal structures. More precisely, the two-shell primary nanocluster *A* in β-Mg_2Al_3 should be considered containing strongly disordered inner shell, while the inner shell of the corresponding nanocluster in $NaCd_2$ is only substitutionally disordered. The outer shell remains ordered in both substances and provides the resemblance of β-Mg_2Al_3 and $NaCd_2$. This difference from the ordered primary nanocluster *A* in $NaCd_2$ is probably caused by the sizes of Mg and Al atoms (smaller and closer to each other) compared to Na and Cd atoms (for elements V_{Mg}/V_{Al} = 23.2 Å^3/16.6 Å^3 = 1.40 vs. V_{Na}/V_{Cd} = 38.2 Å^3/21.6 Å^3 = 1.77). We emphasize that our model naturally interprets the complicated disordering in β-Mg_2Al_3 since all the disordered atoms are allocated in the same inner shell of the primary nanocluster *A*.

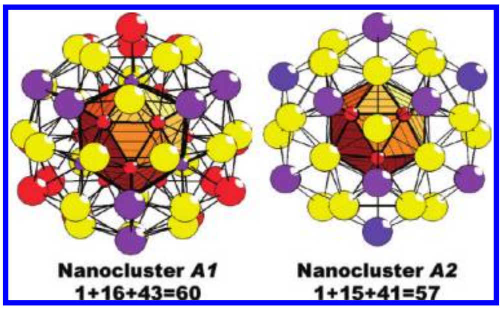

Figure 7. Primary nanoclusters (left) *A*1 and (right) *A*2 in β'-Mg_2Al_3. Blue balls correspond to mixed Mg/Al positions.

β'-Mg_2Al_3. The crystal structure of the low-temperature phase β'-Mg_2Al_3 is a good testing example for the nanocluster approach, since it has 11 inequivalent atoms allocated in the most symmetrical positions 3*a* of the space group *R*3*m* (see Tables 4$-$7 in ref 20), out of which four atoms [Mg(17a), Mg(17b), Mg(18a), Mg(23a)] have maximum coordination numbers (16). Which of them are to be chosen as the centers of nanoclusters? To answer this question we have constructed with TOPOS all models of β'-Mg_2Al_3, where at least one nanocluster is centered with one of the 11 inequivalent atoms and the total number of different nanoclusters does not exceed 8. TOPOS enumerated more than 253 millions of cluster combinations out of which 2973 obey the principles of the nanocluster analysis (see Supporting Information). However, only the model with the cluster centers at Mg(23a), Mg(23b), Al(22a), Al(22b) obeys the parsimony principle best of all; all other models contain more than four nanoclusters. It is the model that is closely related to the model of the high-temperature β-Mg_2Al_3 phase described above. Both

Mg(23a) and Mg(23b)-centered two-shell primary nanoclusters have the same symmetry (3*m*), but they are slightly different by composition (contain 60 and 57 atoms, respectively) and will be called *A*1 and *A*2 to distinguish them from the 61-atom nanoclusters *A* of *β*-Mg_2Al_3 and centered on Mg(23). The primary nanocluster *A*1 is based on a Friauf polyhedron as first shell, but unlike *A*, has one atom less in the outer shell 1 + 16 + 43 = 60 (Figure 7, left). More significant changes are observed for the primary nanocluster *A*2: the inner shell is a 15-atom Frank−Kasper polyhedron *Z*15 with 24 triangular faces, and the outer shell consists of 41 atoms compared to 44 and 43 atoms for the primary nanoclusters *A* and *A*1, respectively (Figure 7, right). Both *A*1 and *A*2 fragments do not occur in the high-temperature phase; they are not the subsets of the primary nanocluster *A*. The 63-atom two-shell Al-centered [Al(22a), Al(22b)] primary nanoclusters are equivalent to the nanoclusters *B* [centered on Al(22)], though having a lower symmetry (3*m* and *m*, respectively).

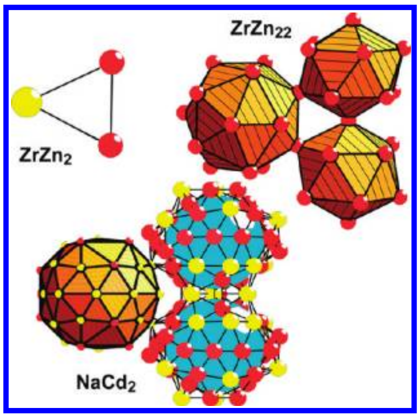

Figure 8. Hierarchical relations between $ZrZn_2$, $ZrZn_{22}$, and $NaCd_2$ supraclusters.

These differences do not influence the method of connecting nanoclusters, self-assembly, or underlying net topology. Thus, the nanoclusters form the supraclusters $A1B_2$ and $A2B_2$ where the pairs *A*1 (*A*2)−*B* and *B*−*B* share one and five external atoms, respectively, *A*1 and *A*2 nanoclusters have no common atoms. We emphasize that the supraclusters have the same symmetry (*m*) as in the high-temperature phase despite the lower symmetry of the structure as a whole; the supraclusters are topologically equivalent in the net. The supraclusters assemble into microchains and microlayers of the topology described in the section "Method of Self-Assembly", finally yielding the underlying 3D net of the $MgCu_2$ topology.

Thus, the phase transition *β* → *β*′-Mg_2Al_3 can be characterized by small changes in the primary nanoclusters *A* that is evidently caused by the structure ordering: half of the nanoclusters retain their inner shell, but lose one atom from the outer shell, whereas another half undergoes a slight reconstruction of both shells.

***β*, *β*′-Mg_2Al_3 versus $ZrZn_{22}$.** The nanocluster approach reveals a similarity in the self-assembly of $NaCd_2$,[6] *β*, *β*′-Mg_2Al_3 and $ZrZn_{22}$.[7] All the phases are composed of triangular AB_2 supraclusters united into the $MgCu_2$-like underlying net, while structure and composition of the primary nanoclusters *A* and *B* could be quite different. The $ZrZn_{22}$ phase can be considered as the first step in the nanocluster growth since both *A* and *B* primary nanoclusters are one-shell in this case and correspond to the inner-shell Friauf polyhedron and icosahedron that are positionally ordered in the crystal structure of $NaCd_2$ (Figure 8). In *β*-Mg_2Al_3 the inner shells of nanoclusters *A* are positionally disordered, while ordering in *β*′-Mg_2Al_3 gives rise to changing inner shells of one-half of *A* nanoclusters to *Z*15 Frank−Kasper polyhedra. The second shell layers over the polyhedra in a little different way in $NaCd_2$, *β*-Mg_2Al_3, or *β*′-Mg_2Al_3, but the packing of the nanocluster centers retains in all cases and

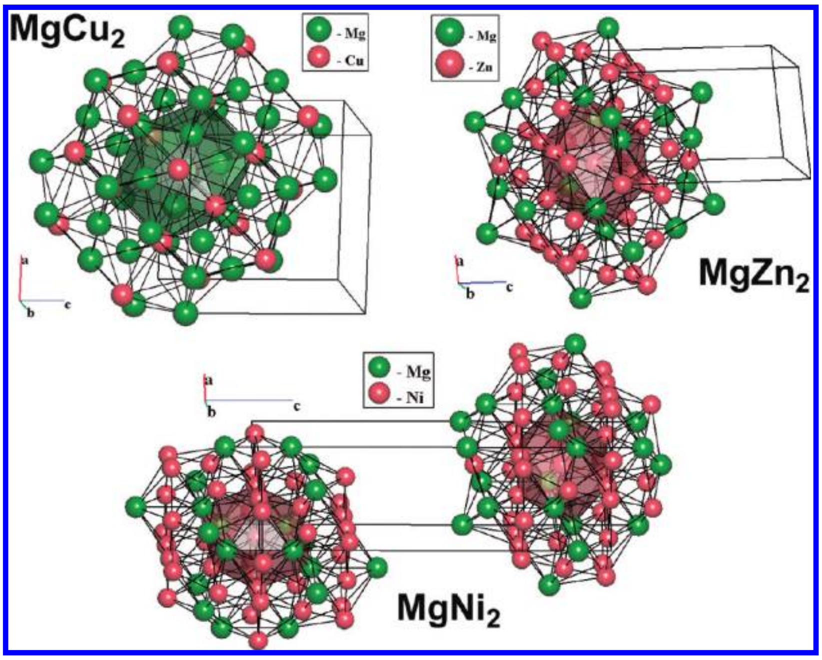

Figure 9. Nanoclusters *B* in the crystal structures of the Laves phases $MgCu_2$, $MgZn_2$, and $MgNi_2$. Internal icosahedra are shown.

corresponds to the $MgCu_2$ motif. Note that there is a $MgCu_2$-like phase in the Zr−Zn system ($ZrZn_2$) that can be considered as the "zero step" of the growth of the nanocluster shells in the sequence $ZrZn_2$ (no shells; clusters are single interconnected atoms) → $ZrZn_{22}$ (one-shell nanoclusters) → $NaCd_2$, β, β'-Mg_2Al_3 (two-shell nanoclusters) (Figure 8).

Primary Nanoclusters *A* and *B* in Other Structure Types. Using the TOPOS procedure of searching for finite fragments in infinite nets[7] we explored more than 27000 intermetallic and related compounds contained in the Inorganic Crystal Structure Database (ICSD, release 2009/2)[29] and Pearson's Crystal Data (PCD, release 2009/10)[30] and found that two-shell nanocluster *B* exists in the Laves phases $MgCu_2$, $MgZn_2$, and $MgNi_2$ and in the structures of 41 other Pearson classes (see Supporting Information). The nanocluster *A* was found only in three Pearson classes: *cF*464 (including $K_{17}In_{41}$,[31] $Na_{17}In_{12}Ga_{29}$,[31] $Li_{18}Cu_5In_4Ga_{31}$,[32] $Na_{35}Cd_{23.77}Ga_{56.23}$,[33] $Mg_{35.07}Cu_{24}Ga_{52.67}$,[34] $Na_{36}Ag_7Ga_{73}$),[35] *hP*238 ($K_{39}In_{80}$),[36] and *cF*5928 ($Al_{56.6}Cu_{3.9}Ta_{39.5}$);[37] the nanoclusters *A*1 and *A*2 occur in β'-Mg_2Al_3 only. Thus, the nanoclusters *A*1 and *A*2 can be considered as "determinants"[6] of β'-Mg_2Al_3. Unlike nanoclusters *A*, the nanocluster *B* is a typical fragment of intermetallic compounds, though it cannot be always considered as a building unit. For instance, in all the Laves phases this nanocluster is much larger than the unit cell; the primary nanoclusters chosen in accord to the principles of the nanocluster analysis are either separate atoms ($MgCu_2$) or an icosahedron ($MgZn_2$ and $MgNi_2$) that is the core of the nanocluster *B*. Nonetheless, the existence of topologically and geometrically similar 63-atom fragments (Figure 9) proves the similarity of the intermetallic phases with large unit cells that is worth exploring in detail separately.

Conclusion

The analysis of $NaCd_2$ and the two phases of Mg_2Al_3 together with previous treatments of the Rh_7Mg_{44} and $ZrZn_{22}$ families[5,7] show that the extremely complicated intermetallic compounds can be modeled with the same principles; moreover, the common approach allowed us to find close similarities in the self-assembly of $NaCd_2$, β, β'-Mg_2Al_3, and $ZrZn_{22}$. The question remains: do the primary nanoclusters exist in the melt, and at which precrystallization stage do they emerge? This question is similar to the problem of searching for relationships between nanoparticles and solids as well as for the ways of their transformation. A possible way to answer this question could be in the study of nanoparticle systems whose size allows application of high-resolution electron microscopy.[38] Mass spectroscopic analysis of alloys as well as computer modeling of nanoparticles could also be informative.[39] However, in any case, the occurrence of the same nanocluster in different crystal structures proves their resemblance and could be an essential criterion for their taxonomy. An important advantage of the proposed analytical procedure is that it is rigorously algorithmized, implemented into a computer program, and, thus, provides a universal and objective approach to modeling of any crystal structure. Since the clusters are of nanosize and contain the number of atoms typical for small nanoparticles, the nanocluster approach can be viewed as a bridge from intermetallic structures to nanoalloys,[39] to cluster-assembled materials[40,41] and to icosahedral quasicrystal approximants.[42−44]

Acknowledgment. V.A.B and G.D.I. thank the Russian Foundation for Basic Research for Grant 09-02-01269.

Supporting Information Available: Table of 44 Pearson classes where nanoclusters *B* were found and the full list of 2973 nanocluster models (maximum number of nanoclusters in a model is restricted to 8) found by TOPOS for β'-Mg_2Al_3. This material is available free of charge via the Internet at http://pubs.acs.org.

---

(29) Belsky, A.; Hellenbrandt, M.; Karen, V. L.; Luksch, P. *Acta Crystallogr*. **2002**, *B58*, 364; http://www.fiz-karlsruhe.de/icsd_home.html.

(30) Villars, P.; Cenzual, K. *Pearson's Crystal Data: Crystal Structure Database for Inorganic Compounds*; ASM International: Materials Park, Ohio, U.S.A.

(31) Cordier, G.; Muller, V. *Z. Naturforsch*. **1994**, *49B*, 721.

(32) Chahine, A.; Tillard-Charbonnel, M.; Belin, C. *Z. Kristallogr*. **1995**, *210*, 80.

(33) Tillard-Charbonnel, M.; Belin, C. *Mater. Res. Bull*. **1992**, *27*, 1277.

(34) Lin, Q.; Corbett, J. D. *Inorg. Chem*. **2004**, *44*, 512.

(35) Tillard-Charbonnel, M.; Chahine, A.; Belin, C. *Z. Kristallogr*. **1993**, *208*, 372.

(36) Lin, Q.; Corbett, J. D. *Inorg. Chem*. **2003**, *42*, 8768.

(37) Weber, T.; Dshemuchadse, J.; Kobas, M.; Conrad, M.; Harbrecht, B.; Steurer, W. *Acta Crystallogr*. **2009**, *B65*, 308.

(38) Talapin, D. V.; Shevchenko, E. V.; Bodnarchuk, M. I.; Ye, X.; Chen, J.; Murray, C. B. *Nature* **2009**, *461*, 964.

(39) Ferrando, R.; Jellinek, J.; Johnston, R. L. *Chem. Rev*. **2008**, *108*, 845.

(40) Talapin, D. V. *ACSNano* **2008**, *2*, 1097.

(41) Shelley, A.; Claridge, S. A.; Castleman, A. W., Jr.; Khanna, S. N.; Murray, C. B.; Sen, A.; Weiss, P. S. *ACSNano* **2009**, *3*, 244.

(42) Lin, Q; Corbett, J. D. *Inorg. Chem*. **2003**, *42*, 8762.

(43) Lin, Q; Corbett, J. D. *Struct. Bonding* (*Berlin*) **2009**, *133*, 1.

(44) Alvarez, S. *Dalton Trans*. **2005**, 2209.